EARTH SURFACE PROCESSES AND LANDFORMS
Earth Surf. Process. Landforms (2017)

Published online in Wiley Online Library
(wileyonlinelibrary.com) DOI: 10.1002/esp.4279

Two new conceptual models for the formation and degradation of baymouth spits by longshore drift and fluvial discharge (Iguape, SE Brazil)

Javier Alcántara-Carrió,[1]* Thaya M. Dinkel,[2] Luana Portz[3] and Michel M. Mahiques[1]
[1] Instituto Oceanográfico, Universidade de São Paulo, São Paulo, Brazil
[2] Facultad de Ciencias, Universidad de Alicante, San Vicente del Raspeig, Alicante, 03690, Spain
[3] Research group in Environmental Management and Sustainability, Faculty of Environmental Sciences, Universidad De La Costa, Calle Barranquilla, Atlántico Colombia

Received 2 September 2016; Revised 5 October 2017; Accepted 19 October 2017

*Correspondence to: Javier Alcántara-Carrió, Instituto Oceanográfico, Universidade de São Paulo, Praça do Oceanográfico 191, São Paulo, SP 05508-120, Brazil. E-mail: javier.alcantara@usp.br

ESPL
Earth Surface Processes and Landforms

ABSTRACT: This study describes the formation of two successive baymouth spits systems on the south-eastern Brazilian coast and the degradation of the first system. The study area includes the Jureia Beach spit, the deflected Ribeira de Iguape River mouth, the central Iguape sandy headland, the Icapara Inlet of the Mar Pequeno Lagoon and the northern end of the Comprida Island barrier spit. The wave and river flow patterns were combined with the coastline evolution and the alongshore migration rates deduced from satellite images. Initially, both spits showed convergent alongshore migration rates equal to or less than 83 m/yr. However, the extreme river flow due to high rainfall during a very strong El Niño event in 1983 eroded the inland side of the Jureia Beach spit, which finally retreated due to wave erosion. In 1989, a sand bank emerged in the river mouth, which attached to the central headland forming a recurved northeastward spit. In 1994, the high fluvial discharge associated with another very strong El Niño event caused the landward migration of the new spit and emersion of a second sand bank. This second sand bank merged with the Jureia Beach spit in 1997 at an alongshore migration rate of 1795.6 m/yr. Wave erosion of the central headland continued and the attached spit disappeared in 2000. In 2009, the headland erosion merged the river mouth and the Icapara Inlet, which resulted in flanking baymouth spits in a configuration that remains today. Therefore, two models for the formation of baymouth spits have been documented for wave-dominated microtidal coasts in humid tropical regions with intense fluvial discharge. The convergent longshore migration of the spits is controlled by both the bidirectional longshore drift and the fluvial discharge, the latter eroding the fronting spit, supplying sediments and acting as a hydraulic blockage for longshore drift. Copyright © 2017 John Wiley & Sons, Ltd.

KEYWORDS: sand barrier; inlet; river mouth; wave; El Niño; hydraulic blockage

Introduction

Coastal barriers generally are composed of sands, gravels, or a mixture of both. They form emerged depositional landforms, usually with a shore-parallel orientation and separated from the mainland by a lagoon, bay or marsh. Coastal barriers are among the most dynamic depositional coastal bedforms, rapidly responding to changes in both the littoral sediment supply and sea level changes, as well as to dynamic processes related to storms (Arnott, 2010; Masselink and van Heteren, 2014).

Several authors have created classification schemes for barrier types. A simple classification was established by Ollerhead (1993), defining three major types of barriers systems on the basis of barrier geometry and the number of free ends: no free end, one free end (including spits), and two free ends (barrier islands). More recently, Otvos (2012) classified barrier systems into process-oriented functional categories: (i) shore-parallel sand and gravel barrier islands, (ii) mainland-attached barrier spits that partially or almost completely enclose bays and lagoons, and (iii) mainland barriers, including beach ridge plains, progradated strandplains, dunefield barriers and cheniers. One of the major geomorphological features of coastal barriers is the inlets. Inlets can be divided into four groups, considering the processes of inlet formation: storm-generated scour channels, spit growth narrowing the entrance of flooded valleys, intersection of major tidal channels by transgressive barrier islands, and tidal-prism controlled (Hayes and Fitzgerald, 2013).

Spits correspond to the second group of coastal barriers, following Otvos (2012). Spits are sediment accumulations that build up above high tide level and diverge from the coast; they usually end in one or more hooks or recurves. They are common morphological features found at river mouths, the end of barrier islands, and inlets (Hoan *et al.*, 2011). They require both a supply of sediment and wave energy to move the sediment, and they commonly occur in areas where there is an abrupt change in shoreline direction, growing in the predominant direction of longshore drift (Schwartz, 1972). Nevertheless, their morphology is controlled by a wide range

of variables such as wave energy and incident angle, tidal and fluvial currents, sediment supply and sea level rise, and other geological factors (Johnson, 1925; Evans, 1942; Redfield and Rubin, 1962; Zenkovich, 1967; O'Brien, 1969; Davis, 2013). In river mouths, the fluvial sediment input into the sea decreases the accommodation space, creating a morphodynamic feedback that is important in the initial stage of spit formation. Exceptional periods of large volumes of sediment discharge during a river flood, often related to climatic variations and anthropogenic influence in the river basin, can drive the initiation of spit formation and its emergence (Dan *et al.*, 2011). The effects of human disturbances such as construction of dams and harbours, urbanization and sand mining can also modify the morphology of spits (Correa *et al.*, 2005; Hanamgond and Mitra, 2008; Orejarena Rondón *et al.*, 2015).

Numerical models can reproduce the growth and elongation of linear and curved spits under a predominant longshore transport (Kraus, 1999; Palalane *et al.*, 2014; Ashton *et al.*, 2016). Simulation of a wave-dominated coast with a river mouth resulted in the development of both a sandy spit and a submarine terrace, the latter was related to the fluvial sediment input, but fluvial blockage was not identified (Kuroiwa *et al.*, 2014). A process-based numerical model was developed to simulate the sediment transport and morphologies in a large deltaic barrier-spit system below the influence of waves, tides, wind and river flow. This model showed that, in a mesotidal environment, the fluvial input of sediments and sediment transport by waves are the basic mechanisms for barrier formation, but river flow counteracts the barrier formation (van Maren, 2005).

This study is focused on baymouth spits (Zenkovich, 1967), a particular category of spits according to the classification of Otvos (2012). Two convergent spits in the mouth of a bay or a river are classified as a double spit (Robinson, 1955; Hume and Herdendorf, 1988), baymouth spits (Zenkovich, 1967) or baymouth barriers (Otvos, 2012). Robinson (1955) attributed elongation of one spit to longshore drift by waves, but could not explain the opposite migration of the counter-drift spit, suggesting that the baymouth spits stemmed from the breaching of a single spit. Ward (1922) and Kidson (1963) observed that paired spits grow in opposite directions. Formation of recurved baymouth spits was described by Zenkovich (1967), who showed that sometimes the baymouth spits can merge and form into a baymouth barrier that closes the bay, with the widest section in the centre of the barrier. Numerical simulation of the formation of symmetric baymouth spits from sandy headlands in both margins of a bay, with an idealized flat seabed, has shown that they extend in straight lines in shallow water, while they are markedly curved inward at the tips when the water is too (Uda and Serizawa, 2011). In addition, asymmetric development was achieved in numerical simulations for different seaward arrangements of the sandy headlands (Watanabe *et al.*, 2014).

The formation and development of double-spits or baymouth spits was first related to longshore drift (Zenkovich, 1967). Numerical modelling has identified a wave-sheltering effect due to the existence of multiple sand spits. Thus, wave energy is reduced when waves pass near the tip of the first sand spit, resulting in the reduction of the wave that reaches the second sand spit (Watanabe *et al.*, 2014). However, it must be noted that, in this modelling, incident waves were propagated from a direction normal to the shoreline, wave refraction was neglected and waves were assumed to propagate in a straight trajectory to maintain a consistent incident angle (Watanabe *et al.*, 2014).

Empirical studies have shown that development of counter-drift spits requires a hydraulic blockage of the longshore drift by tidal currents and/or river flows. Thus, littoral drift in tidal inlets is modulated by hydraulic blockage due to tidal currents (Lynch-Blosse and Kumar, 1976; Hume and Herdendorf, 1993), whereas in wave-dominated microtidal bays and river mouths, littoral drift is modulated by the fluctuations of sediment input and hydraulic blockage due to river flow (Frihy and Lawrence, 2004; Avinash *et al.*, 2013; Hedge *et al.*, 2015). Formation and rapid degradation of convergent baymouth spits have been concisely described in several studies (Frihy and Lawrence, 2004; Liu, 2013). However, few studies have described the formation and development of baymouth spits in detail (Lovegrove, 1953; Robinson, 1955; Aubrey and Gaines, 1982; Carr, 1986; Eddison, 1998; Avinash *et al.*, 2013), and some studies have shown a parallel migration instead of a convergent migration (Raghavan *et al.*, 2001). The objective of this study is to describe the formation of two successive baymouth spits during the recent geomorphological evolution of the Iguape coast [southeast (SE) Brazil], to determine the forcing factors that drive their initial formation, the convergent development and the degradation of the first baymouth spits.

Study Area

The study area is located in the central sector of the São Paulo Bight (SE Brazil). The continental shelf of the São Paulo Bight is one of the widest shelves in the world, with a maximum width of 230 km (Zembruscki, 1979) (Figure 1A). In contrast, the coastal geomorphology of the São Paulo Bight is constrained due to the nearby Serra do Mar mountain chain, closest to the northern sector and farthest to the southern sector. In this littoral mountain chain, Ribeira de Iguape River forms the only major basin on the SE Brazilian coast directly oriented toward the ocean, the river is approximately 470 km long and has a 25 000 km^2 drainage basin area (Besnard, 1950; Muehe, 2012).

Coastal geomorphology of the São Paulo Bight is also controlled by the Late Quaternary relative sea-level changes, which allow the development of coastal plains and estuaries (Suguio and Martin, 1978; Muehe, 2012). The Cananéia estuarine complex is the largest estuarine complex of the São Paulo Bight. It includes the Comprida Island sand barrier and landward Mar Pequeno Lagoon, linked to the ocean by the Cananéia and Icapara inlets (Figure 1B). The channels of the estuary represent the drowning of the paleo-river channels that developed after the transgressive phase of the Isotope Stage 5e (120 000 years bp), locally named the Cananéia Transgression (Martin and Suguio, 1979). Comprida Island is a regressive island 63.5 km long and 5 to 0.5 km wide, essentially composed of Quaternary sandy sediments deposited by a northeastward elongation from a 42-m high hill of Mesozoic intrusive alkaline rocks located at the south-western end of the barrier (Nascimento *et al.*, 2008, Giannini *et al.*, 2009; Guedes *et al.*, 2011). Therefore, the origin of Comprida Island is similar to other barrier spits in Brazil; it is attached to bedrock cliffs or semi-consolidated Pleistocene outcrops (Dillenburg and Hesp, 2009; Hesp *et al.*, 2009; Vital, 2009). In fact, only the northern end of Comprida Island corresponds to a spit, hereafter named the Comprida Island spit.

The study area is a 13.22-km longshore segment (24°35′–24°46′S and 47°33′–47°21′W) that extends from the Comprida Island spit and the associated Icapara Inlet to the Jureia Beach spit, northward of Ribeira de Iguape River mouth. Both spits are straight and follow the general direction of the coastline. In the centre, separating both water bodies and spits, lays the sandy headland of the Iguape lands, composed of Pleistocene deposits (Martin and Suguio, 1979) that artificially became an island in 1852 due to the opening of the Valo Grande Channel, which connected the river course with the inlet (Mahiques *et al.*, 2009) (Figure 1C).

The area is characterized by the alternation of two dominant meteorological systems. On the one hand, there is an inflow of tropical air from the South Atlantic Tropical Anticyclone (SATA)

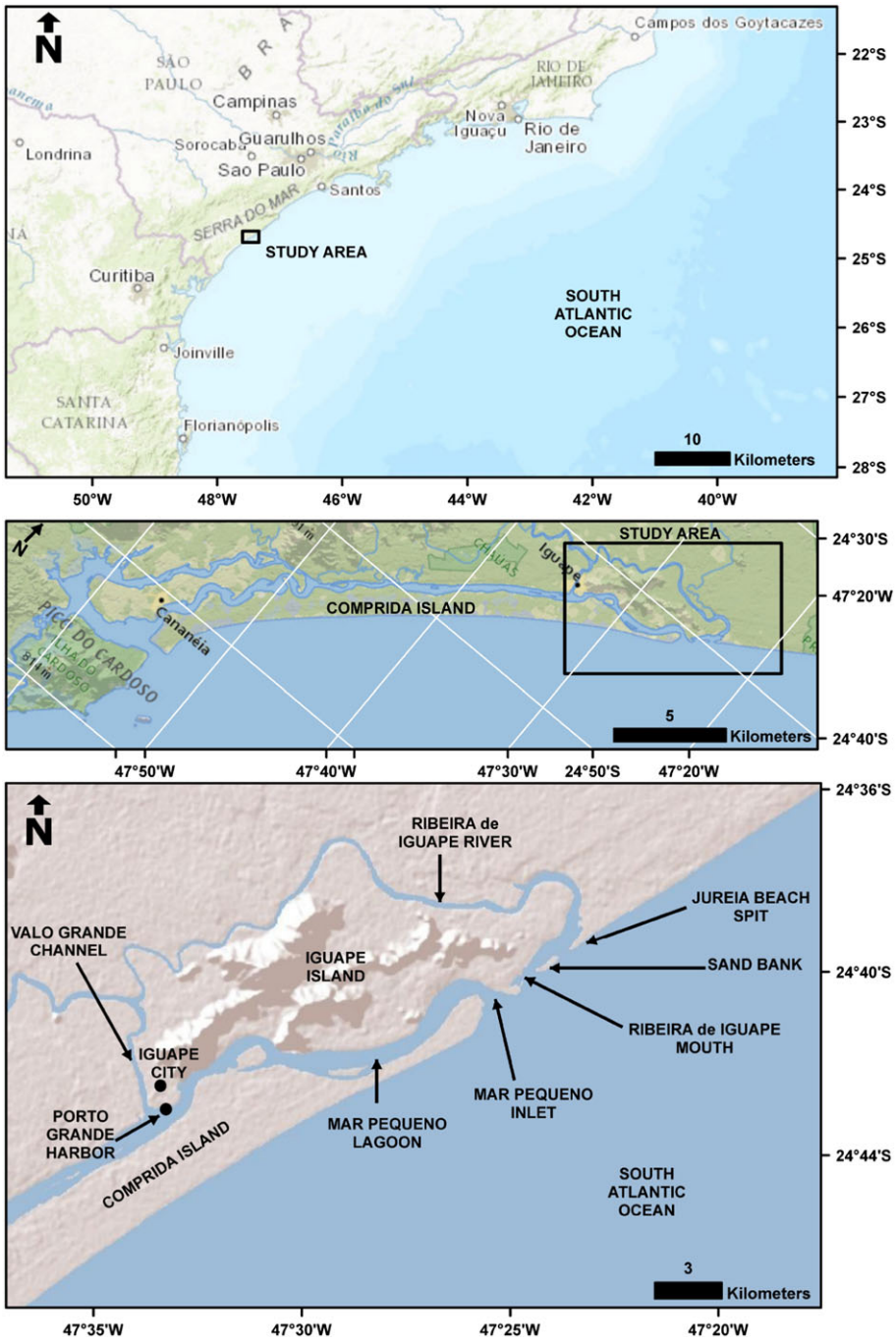

Figure 1. Study area. [Colour figure can be viewed at wileyonlinelibrary.com]

that creates the trade winds throughout the year. On the other hand, the inflow of polar air from the south, the Atlantic Migratory Polar Anticyclone (APM), is followed by frontal systems with associated winds, which are usually more intense during autumn and winter (Nimer, 1989).

The rainfall is characteristic of a subtropical humid climate, with a marked seasonal pattern. In winter and early spring (May–September), rainfall is mainly due to the extra tropical circulation regime due to migratory cyclones along the subtropical Atlantic coast. In the warm season (September–April), rainfall is related to the activity of the South American Summer Monsoon (SASM), which is responsible for more than 80% of the annual mean precipitation in its activity centre (23°S) and for 50% of the total summer precipitation on the coast south of 25°S (Vera *et al.*, 2002; Nagai *et al.*, 2014). As a result of the typical variations in the rainfall pattern, the outflow in the lower course of the Ribeira de Iguape River ranges from 300 to more than 1200 m^3/s (Mahiques *et al.*, 2014).

Two opposite wave approach directions are predominant in the area: the trade winds generate waves from north and northeast throughout the year, while intense winds associated with the cold fronts are responsible for the higher storm waves from the south (Tessler, 1982; Nimer, 1989; Santos, 2005). Reanalysis of the 1979–2000 wave data base generated by the WAVEWATCH III (WW3) model confirms this bimodal pattern in the São Paulo Bight: a typical offshore significant wave height (Hs_o) of 1.5 m and peak period (Tp) of 8 seconds are observed throughout most of the year, but higher Hs_o and longer Tp occur in autumn and winter due to the entrance of cold fronts from the south (Pianca *et al.*, 2010; Silva *et al.*, 2016).

The astronomical tides present a mixed microtidal regime, with amplitudes recorded ranging between 0.25 m during neap tides and 1.2 m during spring tides at the southern end of Comprida Island (Mesquita and Harari, 1983; Guedes, 2009). Flood tidal currents enter the Mar Pequeno Lagoon at different times for the Cananéia and Icapara inlets, converging at its mid-

northeast portion and later diverging from this point during the ebb flows. The propagation of this tidal wave is the main drive of the circulation in this lagoon system, which mixes the oceanic and fresh waters (Bonetti-Filho *et al.*, 1996).

The shore is characterized by dissipative beaches with a rectilinear shape in plan-view and exposed to oceanic waves (Nascimento, 2006). In fact, the Iguape–Cananéia sector contains the most dissipative beaches of the State of São Paulo (Mahiques *et al.*, 2016). A northeastward longshore drift is dominant in the northernmost sector of Comprida Island. Nevertheless, seasonal variations in the longshore drift direction have been described by numerical wave propagation. Thus, a southwestward drift occur in summer and spring, and a northeastward drift in autumn and winter. Moreover, the wave energy is unevenly distributed along Comprida Island, with the highest values in the northernmost sector, reaching up to 220 W/min. Consequently, shoreline in this sector is highly eroded (Silva *et al.*, 2016).

Compared to the northern sector of the São Paulo Bight, coastal human occupation in the area is low or very low (Mahiques *et al.*, 2016). However, human disturbances have caused severe changes in the hydrodynamics and morphodynamics of the area, as well as increased pollution (Mahiques *et al.*, 2009, 2013). The artificial Valo Grande channel was opened 30 km upstream of the Ribeira de Iguape River mouth, connecting the river course to the Mar Pequeno lagoon to reduce the navigation distances to Porto Grande Harbour, at that time one of the most important export harbours of the Brazilian Empire. The construction of the channel started in 1827 and finished in 1852. The initial dimensions were 4 m wide and 2 m deep. However, due to the fast erosion of the unconsolidated sediments on its riverbanks, the channel reached 100 m wide and 10 m deep at the end of the nineteenth century (Geobrás, 1966), and it was 300 m and an average of 7 m deep in 2009 (Mahiques *et al.*, 2009). After the opening of the Valo Grande, river discharges flowed to both outlets equally or as much as two-thirds of the original river flow was diverged to the Mar Pequeno lagoon (Geobrás, 1966). It has been estimated that, between 1852 and 1911, the Valo Grande channel discharged up to 4 200 000 m^3 of eroded sand from the Iguape River to the Mar Pequeno lagoon (Geobrás, 1966). These large inputs of sediments created sandbanks at the outlet of the artificial channel. Tidal currents were not strong enough to distribute the sediment causing accumulation at the Porto Grande Harbour, which became inaccessible and therefore is no longer functional. Moreover, a series of sand banks emerged in the inner part of the lagoon system (Tessler and Furtado, 1983; Mahiques *et al.*, 2014). The partial diversion of the river course by the Valo Grande artificial channel was temporarily interrupted in 1978, when a dam was built, but in 1983, intense rains and floods related to an El Niño event allowed the dam to open again (Mahiques *et al.*, 2009).

As a result of the meteo-oceanographic pattern, sediment supply, geological framework and human disturbance, the elongation of the Comprida Island spit has continued, with the consequent northward migration of the Icapara Inlet and erosion of the coastal plain. According to Pimentel (1762), the Icapara Inlet was located 8.3 km away from the Ribeira de Iguape River mouth in 1721. Analysis of nautical charts, historic maps, aerial photographs and field observations allow the deduction of an average elongation rate of the Comprida Island spit of 35 m/yr from 1882 to 1964, and the southern margin of the central sandy headland simultaneously retreated at 32 m/yr (Geobrás, 1966; Tessler and de Mahiques, 1993). More recently, analysis of aerial photographs and satellite images from 1962 to 2000 by Nascimento *et al.* (2008) showed an average rate of 27.5 m/yr, which does not agree with an average rate of 15.5 m/yr from 1976 to 2000, as deduced by Kawakubo (2009) from the analysis of four satellite images. Two main theories support the relatively high migration rates of the northern end of the Comprida Island. Nascimento *et al.* (2008) attributed a greater importance to the artificial Valo Grande channel, indicating that migration of the Comprida Island margin and Icapara Inlet was significantly favoured by the river discharge coming from this artificial channel; Kawakubo (2009) and Silva *et al.* (2016) related the relatively high migration rates to the predominant southerly waves and resulting northeastward littoral drift.

However, an ancient undated channel shift in the Ribeira de Iguape River course, changing from a northeastward to southwestward direction, was identified by Bentz and Giannini (2003). These authors also proposed a fluvial hydraulic blockage of the longshore drift associated with dominant southerly waves in the present Ribeira de Iguape River mouth, as well as in the Una do Prelado River mouth, 43 km away, in the opposite margin of Jureia Beach. Therefore, the high southwestward elongation of the Jureia Beach spit from 1973 to 2000 could be explained by this ancient mouth relocation and the inversion of the longshore drift along a great extension in the southern sector of Jureia Beach, due to the hydraulic blockage (Bentz and Giannini, 2003). In fact, the analysis of satellite images by Kawakubo (2009) showed an average elongation rate of 24 m/yr from 1976 to 2000.

Material and Methods

Offshore wave data at 25.5°S and 45°W were extracted from the global wave generation model WW3® [National Oceanic and Atmospheric Administration (NOAA)/National Centers for Environmental Prediction (NCEP) – http://polar.ncep.noaa.gov/waves/CFSR_hindcast.shtml] for a 10-year interval (March 2005–March 2015). Annual and seasonal directional wave histograms were created considering the significant wave height (Hs_o) in metres, peak period (Tp) in seconds and mean wave approach direction in degrees with the Grapher™ 8 (Golden Software). The annual histograms included all the data, while the data for the seasonal histograms were obtained according to the meteorological seasons (Trenberth, 1983). Moreover, directional wave histograms were created for the extreme wave regime that included wave heights greater than 2 m (Silva *et al.*, 2016). Furthermore, to determine the frequency of each wave approach direction, percentage tables were created relating the significant wave heights and main directions on both the annual and seasonal scales.

Monthly river flow data (in m^3/s) of the Ribeira de Iguape River from 1976 to 1999 were obtained from a control station located at 24°29′27″S and 47°50′12″W. Maximum flows were identified and related to atmospheric conditions. Moreover, the river discharge was contrasted with the offshore wave patterns to analyse the interaction between them and their influence on the geomorphological evolution of the sedimentary system.

The Multivariate ENSO (El Niño Southern Oscillation) Index (MEI) developed by Wolter and Timlin (1993) and the Southern Oscillation Index (SOI) were considered to determine the occurrence and magnitude of the El Niño events (positive MEI; negative SOI values) and their relationships with the river flow data. Moreover, both indexes were compared by lineal regression, and the correlation coefficient was determined.

Analysis was conducted using a series of 73 satellite images from the satellites LANDSAT-1, LANDSAT-2, LANDSAT-3, LANDSAT-5, LANDSAT-7, CBERS-2, CBERS-2B and IRS-P6, supported by the Brazilian National Institute for Space Research (INPE). The characteristics of each satellite and the

resolution of the images are shown in Table I. These images cover a range of 37 years (1976–2013) and vary from 80 to 30–20 m resolution; the data accuracy has clearly improved since 1984. No images could be used from 1978, 1981, 1983 or 1988, since they had complete or partial cloud coverage. The valid images were geo-referenced with the Autodesk Raster Design 2010.

Initially, the images were used to identify the main bedforms and to describe their general evolution through visual inspection. Later, the detailed 1976–2013 evolution of the bedforms was characterized by the morphometric analysis of the alongshore evolution of their limits and the area of the central headland, according to the method of Aubrey and Gaines (1982). These measurements were carried out by using the Measure Tool of the Surfer™ 11 (Golden Software), according to the following procedure. First, a 13.21-km long straight line was defined alongshore from point A (24°42′21.27″S, 47°28′35.34″W) to point B (24°38′25.55″S, 47°22′2.64″W), in the southern and northern margins of the study area, respectively. Second, six alongshore limits were established over the reference line, according to the borders of the different bedforms. Limit 1 marks the end of the Comprida Island spit; limits 2 and 3 define the southern and northern ends of the central headland, respectively; and the alongshore limit 4 defines the southern end of the Jureia Beach spit. Limits 5 and 6 were defined to the northern and southern end of the two temporary sand banks that emerged inside the Ribeira de Iguape River mouth at different times. Therefore, limits 1 and 2 define the width of the Icapara Inlet, while limits 3 and 4 refer to the width of the Ribeira de Iguape River mouth (Figure 2). Third, distances 1–6 (i.e. distance from point A to limits 1–6, respectively) were measured for each satellite image and plotted with Grapher™ 8 (Golden Software), to identify the evolution of each bedform. Later, the study period was divided into intervals that delineate pronounced variations in at least one of the limits.

Due to the various shape changes in the sandy headland, its area was measured from a second reference line, which was landward and parallel to the first one (Figure 2). The evolution of this area (in m^2) was monitored by the same Measurement Tool of the Surfer® 11 (Golden Software) and the data were plotted with Grapher™ 8 (Golden Software) for the complete time series.

Total migration rates were calculated to describe the evolution of each limit, considering the difference between their initial and final distances from point A and the corresponding dates. Thus, a time span of 36.86 years was applied, since the first image corresponds to 26 June 1976 and the last image corresponds to 5 May 2013. Furthermore, migration rates were also obtained for each period. The sign of the migration rates indicates the direction of displacement, with positive values indicating a northeastward migration and negative values indicating a southwestward migration. Finally, mean migrations rates were obtained for the limits of the spits and the headlands, considering the absolute values of the migration rates for each period.

Table I. Main characteristics of the satellites and resolution of the processed satellite images

Satellite name	Orbit height (km)	Repeat cycle (days)	Resolution (m)	Swath width (km)	Spectral band	Onboard sensor	Launching date	Deactivation Date
LANDSAT-1	920	18	80	184	6	MMS	23 July 1972	6 January 1978
LANDSAT-2	920	18	80	184	6	MMS	22 January 1975	25 January 1982
LANDSAT-3	920	18	80	184	6	MMS	5 March 1978	31 March 1983
LANDSAT-5	705	16	30	185	4 and 5	TM	1 March 1984	5 June 2013
LANDSAT-7	705	16	30	185	4 and 5	ETM	15 April 1999	Operating
CBERS-2	778	26	20	113	4	CCD, IRMSS and WFI	21 October 2003	Late 2007
CBERS-2B	778	26	20	113	1 and 4	CCD, HRC and WFI	17 September 2007	10 May 2010
P6	817	24	23.5	141	4	LISS-III	17 October 2003	Operating

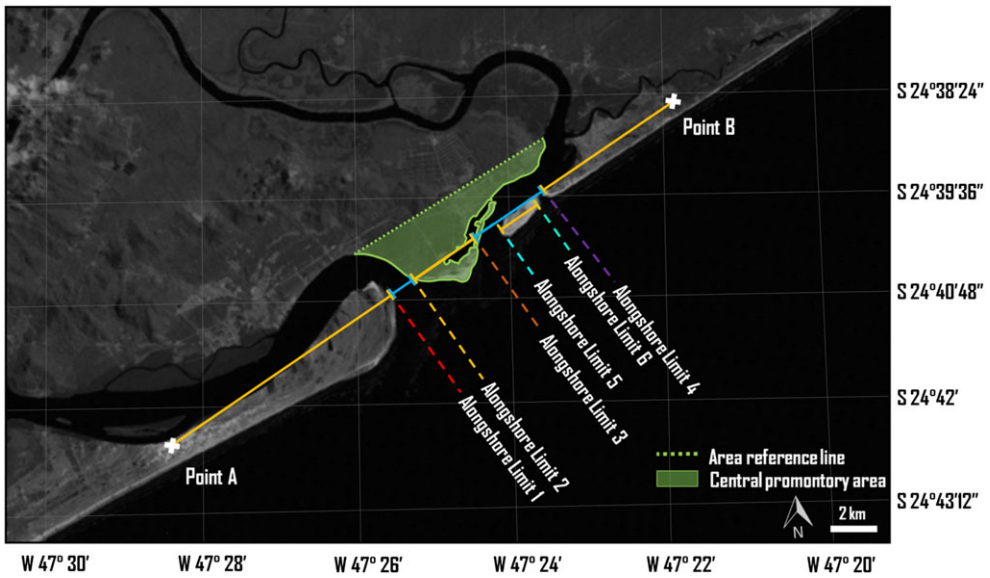

Figure 2. Reference points, lines and alongshore limits to measure the evolution of the bedforms. [Colour figure can be viewed at wileyonlinelibrary.com]

Results

Wave regime and river discharge

The offshore wave distribution showed a bimodal mean wave regime for the annual analysis, with the predominance of waves approaching from the south to south-southwest (S-SSW) (44%) and the east to east-northeast (E-ENE) (31.3%), while a smaller percentage of waves approached from the southeast (SE) (19.9%), northeast (NE) (3.5%) and southwest (SW) (1.1%). The wave heights (Hs_o) ranged between 0.6 and 5.3 m, while the peak period ranged between 4.6 and 15.8 seconds, corresponding to swell waves (Tp $>$ 9 seconds) of the S-SSW component and wind sea waves (Tp $<$ 9 seconds) mainly of the E-ENE component (Figures 3A and 3B). This bimodal behaviour was maintained during the spring and summer mean wave regimes, with an almost equitable distribution between the E-ENE and S-SSW components, slightly dominated by the former. In contrast, the mean wave regime during the winter was mainly from S-SSW, but showed a light bimodal character due to the entrance of the E-ENE waves. Finally, the mean wave regime during the autumn was unimodal, again with dominance of S-SSW waves.

The wave heights higher than 2 m represented 44.5% of the wave data series, showing another bimodal distribution for the extreme wave regime in the annual analysis, with predominance of the S-SSW component (77.4%). The highest storm waves (Hs_o $>$ 4 m) corresponded to swell waves (Tp $>$ 9 seconds) approaching from S-SSW. Storm waves from the E-ENE were rare and related to low peak periods. Extreme waves did not occur in the same proportions throughout the year, they were primarily related to winter (32.2%), followed by spring and autumn with a similar representation (27.7 and 25.5%), and the lower presence during the summer (14.6%).The storm wave regime presented a unimodal S-SSW wave approach direction at both the annual (Figures 3C and 3D) and seasonal scales, except for spring, where an E-ENE component was also significant. This E-ENE storm wave component can also be identified in the summer and winter, at a very low frequency.

The mean annual river flow ranged from 282 to 890 m^3/s, where the highest value corresponded to 1983, and the high flows occurred in the last years of the database, i.e. 1993– 1999 (Figure 4A). Mean monthly river flows in the summer and spring ranged between 166 and 1156 m^3/s (Figure 4B), while it ranged between 187 and 1754 m^3/s in the winter and fall (Figure 4C). The average values were similar for both intervals (483 and 449 m^3/s, respectively). High mean monthly flow values (over 600 m^3/s) mainly occurred in the summer or spring (Figure 4B), but the highest value corresponded to the winter of 1983, with a maximum of 1754 m^3/s.

The most intense El Niño events of the entire 1951–2017 MEI series occurred in 1982–1983 and 1997–1998. In addition, 1986–1988, 1991–1993, and 2009–2010 also correspond to some of the eight strongest El Niño events of the period, according to the MEI (https://www.esrl.noaa.gov/psd/enso/mei/elnino.png). Similarly, the SOI also shows that very strong El Niño events occurred in 1983, 1992 and 1998 (http://www.cpc.ncep.noaa.gov/data/indices/soi), despite the statistical correlation obtained between the MEI and SOI series is null (R^2 = 0.00).

Geomorphological evolution

The study area shows intense morphological changes. At the beginning of the study period (1976), the narrow river and lagoon mouths were separated 2378 m by the central sandy headland, which had a rectangular shape (Figure 5A). In 1985, the headland shape was significantly changed, with a decreased area at the north-eastern margin, while the Jureia Beach spit thinned (Figure 5B). From 1985 to 1989, intense erosion occurred in both

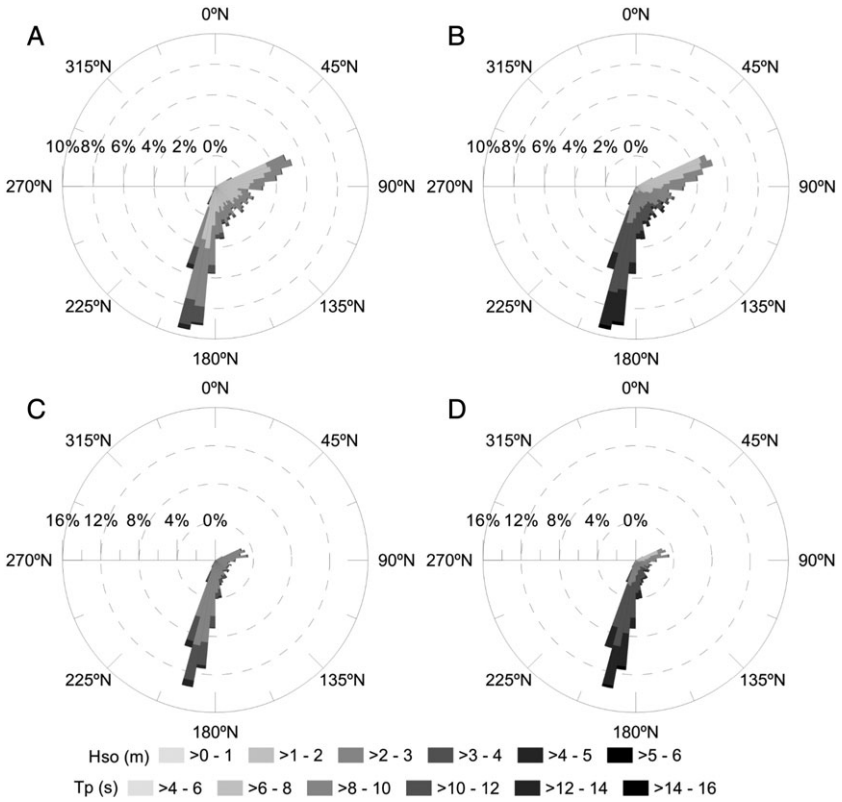

Figure 3. Directional wave histograms over the 10-years period (March 2005 to March 2015): (A) offshore significant wave height and (B) peak period for mean regime; (C) offshore significant height and (D) peak period for storm regime.

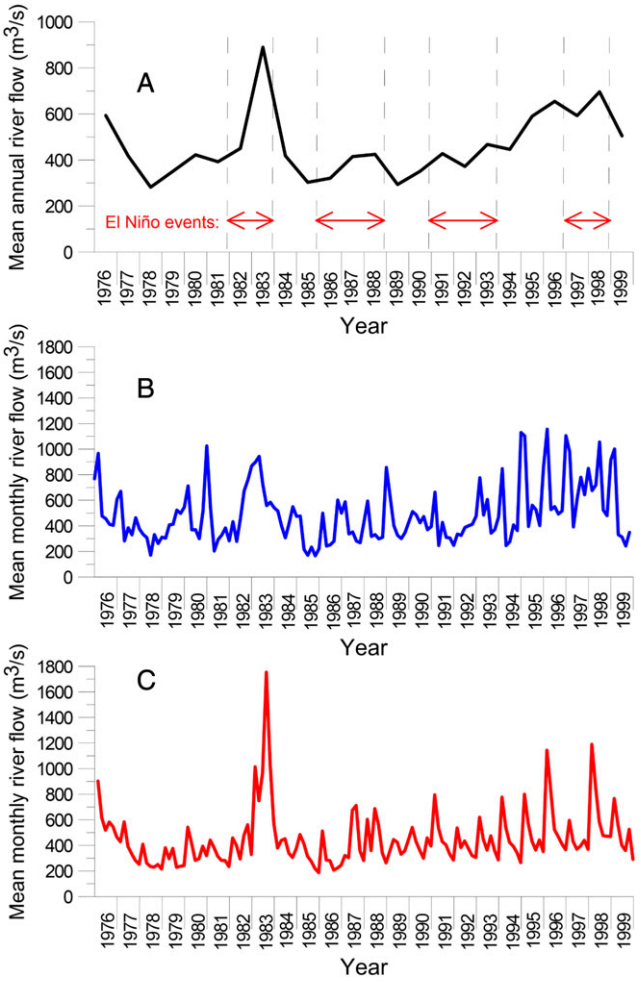

Figure 4. Fluvial discharge (m3/s): (A) mean annual river flow and ENSO events, (B) mean monthly river flow for summer and spring, and (C) mean monthly river flow for winter and autumn. [Colour figure can be viewed at wileyonlinelibrary.com]

the northeast side of the headland and Jureia Beach spit, leaving a very wide river mouth in which a sand bank emerged in 1987 (Figure 5C). Then, in 1989, the first baymouth spits system was developed in the Ribeira de Iguape River mouth, after the sand bank became attached to the headland and its elongation northeastward into the river mouth (Figure 5D). In 1994, a second sand bank emerged close to the Jureia Beach spit (Figure 5E), and these two bedforms attached in 1997 (Figure 5F). Next, from 1997 to 2008, the headland reshaped into a triangular form, while its northward spit disappeared in 2000. The Ribeira de Iguape River mouth migrated southwestward, but it narrowed due to continued southwestward migration and widening of the Jureia Beach spit (Figure 5F). Severe erosion and shoreline retreat of the headland occurred; then, in 2009 the Ribeira de Iguape River mouth and Mar Pequeno Lagoon directly attached, allowing the formation of a second baymouth spit, which was maintained until 2013 (Figure 5G) and is still present.

Nine periods were defined according to the pronounced changes in at least one of the geomorphological units (Table II and Figure 6). Period 1 corresponded to the longest time span, 9.1 years, while Period 5 was the shortest, 0.7 years. Period 9 began in 2009, when the central headland retreated behind the longshore reference line, and therefore, the headland limits were not monitored during this period.

The Comprida Island spit and the southern end of the headland showed a nearly parallel evolution in their northeastward migration, related to the growth of the spit and the erosion of the southern end of the headland (Figure 6). Therefore, the width of the Icapara Inlet varied between 276.0 and 1045.5 m. In contrast, the Jureia Beach spit and the northern end of the headland reflected a non-parallel evolution and had more pronounced variations, with intense northeastward migration between 1985 and 1989 (period 2) and between 1989 and 1991 (period 3) for the spit and the northern end of the headland, respectively; the width of the headland therefore increased, while the Jureia Beach spit eroded. In addition, a regular southwestward migration trend was identified for both the northern end of the headland and the Jureia Beach spit, from 1976 to 1985 (period 1) and from 1997 to 2013 (periods 6–9), associated with erosion of the headland and elongation of the spit. As a result, the width of the Ribeira de Iguape River mouth varied in a wider range, from 174.2 to 2546.3 m, than that of the Icapara Inlet.

Emerged sand banks appeared from 1987 to 1988 (period 2) and from 1994 to 1996 (period 4). In both cases, due to the low temporal resolution, they were several hundred of metres long when they were first recorded. Both sand banks later joined one of the major bedforms. The first sand bank attached to the northern end of the headland in 1989, and the second sand bank attached to the Jureia Beach spit in 1997, causing an elongation of 1259.4 m.

In general, the system followed a longshore migration pattern, where both spits progressively converged, eroding the headland that separated their associated drainages. This pattern was followed in the beginning (1976–1985) and in the end of the studied period (1997–2013). However, the highly dynamic evolution from 1985 to 1997 seems to describe a non-expected behaviour, considering the relatively uniform and simple convergent trend that followed for 25 years.

The central headland is composed of exposed late Pleistocene (Isotope Stage 5e) sandy deposits, containing fossil tubes of *Callichirus major* (Suguio and Martin, 1976) at 0.5 m above the present mean sea level, as observed during fieldtrips to the seaside. The headland area decreased following a regular pattern without abrupt changes from 1976 to 1989 (Figure 7). In contrast, from 1989 to 1991, its area increased, related to the merging of the first sand bank in 1989. After that, there was another decreasing trend in the headland area, indicating an ongoing erosion of the headland. In total, 1798.33 $\times$ 10^3 m^2 of the headland area was eroded between 1976 and 2013. Considering the length of 4650 m for the landward reference line employed to determine the area of the headland, this erosion corresponds to an average shoreline retreat of 386.7 m in 37 years, i.e. 10.4 m/yr in a cross-shore direction. Moreover, from 1976 to 2009, the northern and southern margins of the headland migrated 1016.7 and 800.1 m alongshore, respectively, with longshore migration rates of 31.0 and 24.4 m/yr.

Total migration rates, i.e. considering only the initial and final stages, of both spits and the margins of the central sandy headland were quite similar, ranging between 24.4 and 31.0 m/yr, with slightly lower values in the southern sector (Table III). However, in terms of the nine defined periods, the migration rates revealed a more complex system dynamics. Thus, the fastest migration rate was recorded for the Jureia Beach spit, with 1795.6 m/yr during period 5 (1996–1997), corresponding to the merging of the second sand bank with the spit. The second fastest migration rate was 726.5 m/yr, for the northern margin with the headland during period 3 (1989–1991), associated with its merging with the first sand bank. In contrast, the Comprida Island spit and the southern margin of the headland showed the lower maximum migration rates, with 129.1 and 68.3 m/yr, respectively. The mean migration rates were also clearly higher in the northern sector, with 67.7 m/yr for the spit and 58.4 m/yr for the margin of the headland, than in the southern sector, with 22.2 and 24.2 m/yr respectively (Table IV). Therefore, although the total migration rates for all limits were similar (Table III), the Jureia

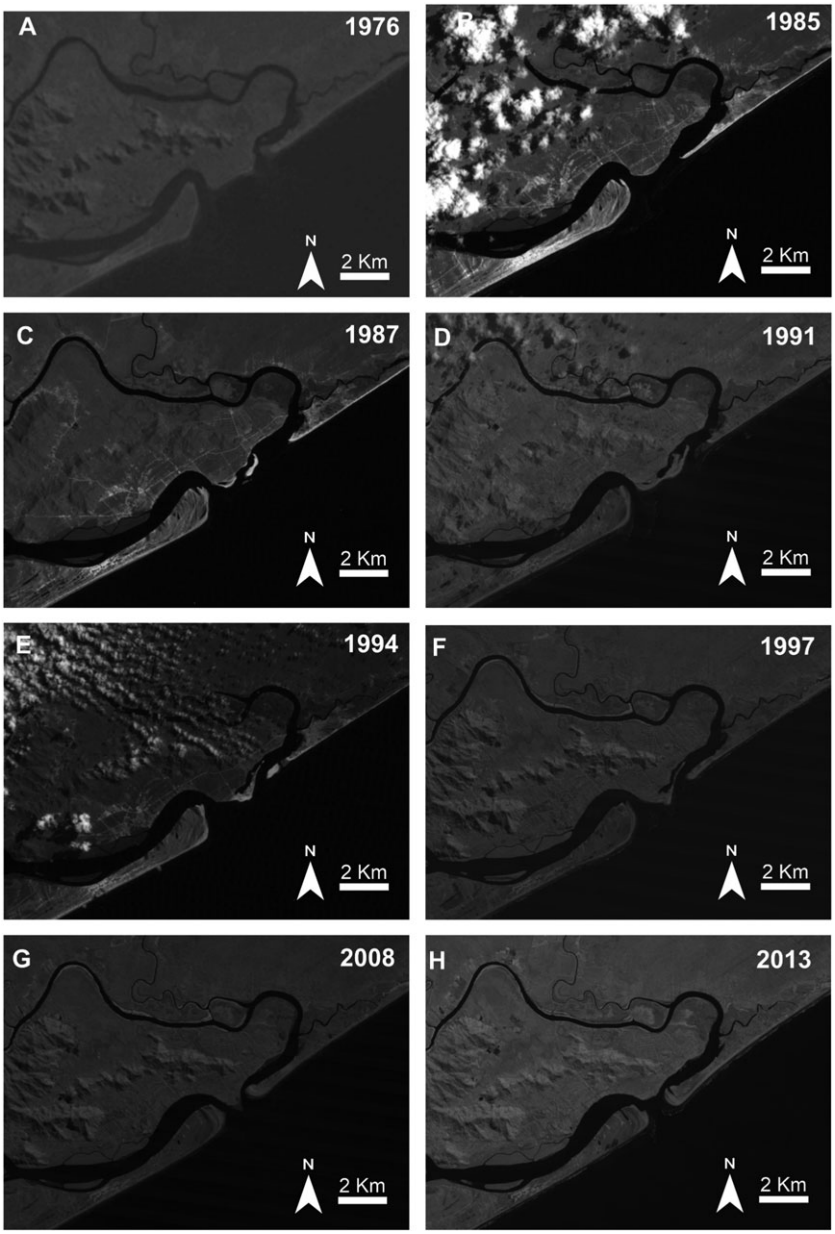

Figure 5. Sequence of satellite images (1976-2013) selected according to some of the major geomorphological changes observed (Source: INPE).

Beach spit and the northern margin of the headland were more dynamic throughout the entire period (Table IV). Moreover, the higher migration rates of the northern sector during the 1985–1997 interval corresponded to the periods 3 and 5, for the northern margin of the headland and Jureia Beach spit, respectively, reflecting the high dynamics of the system in this interval.

Discussion

The offshore mean wave regime in SE Brazil (26°S and 45°W) was described by Pianca *et al*. (2010) and Silva *et al*. (2016). The present analysis at another point, closer to the study area, confirms the bimodal pattern of the mean wave regime at both the annual (Figures 3A and 3B) and seasonal scales, except for

Table II. Duration (years) of each period and related longshore migration (m) of the spits and margins of the central headland

		Longshore migration (m)			
Period	Duration (years)	Ilha Comprida spit	Southern margin of the headland	Northern margin of the headland	Jureia Beach spit
1	9.1	370.2	394.6	–672.1	–756.9
2	3.46	109.2	–3.3	–489.9	1882.2
3	2.37	–73.4	–161.7	1719.1	105.6
4	5.35	96.6	269.6	–840.6	–100.5
5	0.7	58.6	26.2	–3.6	–1259.4
6	2.21	277.4	–27.7	–150.4	–284.7
7	6.32	69.9	318.9	–440.6	–294.1
8	3.31	96.7	–16.5	–139.3	–102.7
9	4.04	15.0	—	—	–211.6

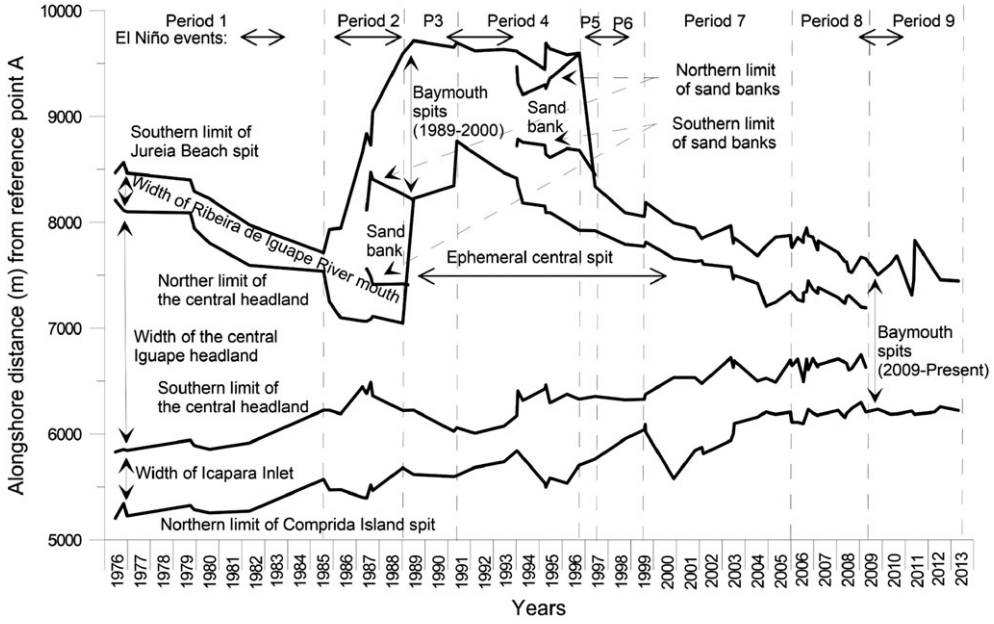

Figure 6. Evolution (1976-2013) of the bedform limits and definition of 9 time periods to calculate the migration rates. ENSO events are showed in the top.

the autumn, where only the S-SSW wave approach direction was significant. In contrast, the storm wave regime shows a unimodal S-SSW wave approach direction for both the annual (Figures 3C and 3D) and seasonal scales, except for spring, where the E-ENE component was also significant. All of these wave analyses are based on the WW3 numerical model. Several authors (Tolman *et al.*, 2002; Pianca *et al.*, 2010) showed that, compared to buoy measurements, this model overestimates the wave heights by approximately 10%. Moreover, in the particular case of SE Brazil, they show a lower range of wave approach directions than the data recorded at a local buoy (Alcántara-Carrió *et al.*, 2017). However, the available buoy wave records in SE Brazil still cover a short period (2011–2017) and therefore, the WW3 model currently supplies the best database for the offshore wave characterization in the region.

The net annual northeastward longshore drift, with a lower southwestward drift in the summer and spring, was obtained after wave propagation for Comprida Island (Silva *et al.*, 2016). A similar drift pattern is assumed to correspond to the study area, because the northern end of the island is included in the study area. Thus, the S-SSW waves favour the northeastward elongation of the Comprida Island spit, as well as erosion of the Jureia Beach spit, while the E-ENE waves favour the opposite process, i.e. southwestward elongation of the Jureia Beach spit and retreat of the Comprida Island spit. However, the convergent longshore migration of the spits, and even more the southwestward net migration of the Jureia Beach spit, cannot be explained exclusively by the longshore drift, as it shows a predominant northeastward direction. Therefore, the river discharge must be considered as an additional controlling factor of the system. Geobrás (1966) suggested that the river flow rates were similar in both the natural course and Valo Grande channel. However, the severe morphological changes identified in the Ribeira de Iguape River mouth, in contrast to the simple evolution of the Icapara Inlet (Figure 6), indicate that the river discharge and sediment supply are mainly flowed through the natural course, at least from 1976 to 2013.

The fluvial discharge produces the hydraulic blockage of the northeastward longshore drift and prevents erosion of the Jureia Beach spit by the southerly waves (Bentz and Giannini, 2003). Considering the wave and river patterns, it can be expected that, during the summer and spring, river discharge interferes with the longshore drift approximately equitably in both directions, and thus, no sediment transport direction is favoured. In contrast, river discharge in the winter and fall should play a major role due to its interference with the dominant northeastward longshore sediment transport by the southerly waves, and the rarity of the eastern waves in these seasons. A similar blockage should be expected to occur at the central headland, due to the hydraulic discharge from the Icapara Inlet.

The highest fluvial discharge of the available time series corresponds to a very strong El Niño event during the winter of 1983 (Figure 4). This extreme rainfall event did not generate an immediate change in the extension of the Jureia Beach spit, but its width significantly decreased due to strong erosion on

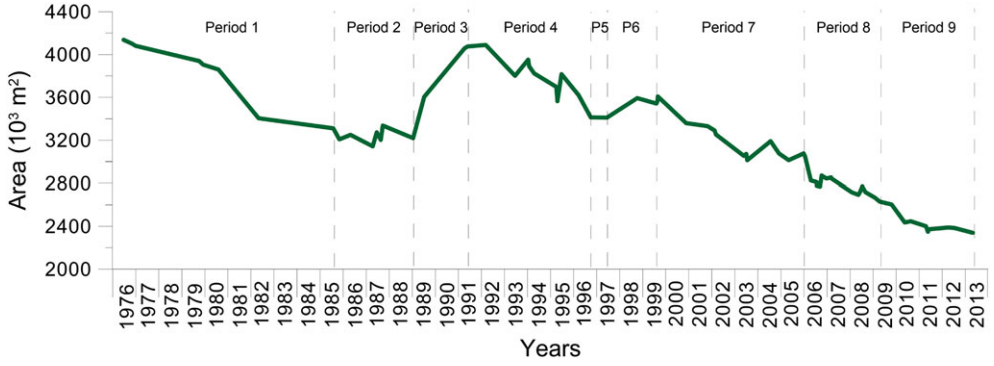

Figure 7. Evolution (1976-2013) of the central sandy headland area (103 m2). [Colour figure can be viewed at wileyonlinelibrary.com]

Table III. Total migration (m), distances and total-period migration rates (m/year) of the spits and margins of the central headland from 1976 to 2013

	Ilha Comprida spit	Southern margin of the headland	Northern margin of the headland	Jureia Beach spit
Total longshore migration (m)	1022.4	800.1	–1016.7	–1022.0
Total duration (years)	36.9	32.8	32.8	36.9
Longshore migration rates (m/yr)	27.7	24.4	–31.0	–27.7

the inner side (Figure 5B). Later, the seaside of the Jureia Beach spit was substantially eroded (Figure 5C), which was probably related to the fact that low river discharge from 1984 to 1985 (Figure 4) was not acting as a hydraulic blockage, permitting a more effective wave erosion by the southerly waves and northeastward longshore drift. River discharge remained relatively low from 1985 until 1992 (Figure 4), permitting a net northeastward longshore sediment transport, which prevented the southwestward migration of the Jureia Beach spit, and generated accretion on its inner part, likely related to both the marine and fluvial sediment inputs. Simultaneously, a sand bank appeared in the northern mouth in 1987, favoured by this low river discharge (Figure 5C). This sand bank merged with the central headland in 1989, transforming into a spit morphology inside of the river mouth, which was evidence of the predominance of the northeastward sediment transport and a low river discharge (Figures 5D and 6). Therefore, the river mouth was flanked by baymouth spits.

The fluvial discharge again intensified from 1993 to 1999 (Figure 4), also related to a very strong El Niño period. Increase in the fluvial discharge decreased the net northeastward sediment transport and consequently, it prevented the development of the central spit inside of the river mouth and reshaped the headland into a triangle (Figures 5E and 5F), simultaneously decreasing the headland area (Figure 7). The rapid diversion and degradation of this new central spit by the river flow is evidence of the low northeastward littoral drift during this period, according to Aubrey and Gaines (1982). Moreover, in 1994, a second sand bank emerged close to the Jureia Beach spit, likely associated with the fluvial inputs and the relative increase in the southwestward sediment transport to this spit (Figures 5D and 5F).

High river discharge in 1983 and 1993–1999 generated different effects. The first event occurred five years after the temporary closure of the Valo Grande channel by a dam (Mahiques *et al.*, 2009). Consequently, the highest river flow of the available series was only canalized by the natural river course, causing high inland erosion of the large Jureia Beach spit, which presented a deflected configuration (Nienhuis *et al.*, 2016). In 1987, the sediments from the eroded spit formed a sand bank that was attached to the central promontory by 1989, forming a recurved spit with two horns (Figure 5D); the northeastward alongshore migration rate reached up to 725.7 m/yr. In contrast, three very different conditions occurred in the 1993–1999 period. First, the river mouth presented a semi-deflected configuration, an intermediate case between the deflected and undeflected cases identified by Nienhuis *et al.* (2016). Second, the Valo Grande channel was open and so part of the flow was diverted by this channel to the Icapara Inlet. Third, and also important, the intense fluvial discharge was not concentrated in a maximum peak period, but it was distributed throughout the entire year (Figure 4). Consequently, river flow erosion was lower because the Jureia Beach spit was shorter and the energy of the river flow was lower. Nevertheless, the hydraulic blockage throughout the entire year favoured the emersion of the second sand bank, which merged to the Jureia Beach spit in 1997, resulting in the highest alongshore migration rate measured in the system (1795.6 m/yr), due to the spit elongation (Figure 6).

Table IV. Detailed Migration rates (m/year) of the spits and margins of the central headland for each period, average migration rates and standard deviation

	Longshore migration rate (m/yr)			
Period	Ilha Comprida spit	Southern margin of the headland	Northern margin of the headland	Jureia Beach spit
1	40.7	43.3	–73.8	–83.0
2	31.5	–1.0	–141.4	543.1
3	–31	–68.3	726.5	44.6
4	18.1	50.4	–157.1	–18.8
5	83.6	37.3	–5.1	–1795.6
6	129.1	–12.9	–70.0	–132.6
7	10.8	49.4	–68.2	–45.5
8	29.8	–5.1	–42.9	–31.7
9	3.7	—	—	–52.3
Mean	22.2	24.2	58.4	67.7

This hydraulic blockage of the longshore drift is similar to that proposed by Lynch-Blosse and Kumar (1976) in tidal inlets of sand barriers. The Icapara Inlet is the mouth of the Mar Pequeno Lagoon in the Cananéia Estuary, where the water circulation is controlled by tidal currents (Bonetti-Filho *et al.*, 1996). However, the high magnitude of the morphological changes in the Ribeira de Iguape River mouth contrast the stable shape of the Icapara Inlet and Mar Pequeno Lagoon; only small changes were observed in the sand banks inside Icapara Inlet. The development of a temporary spit, associated with dominance of the southerly waves, in the northeast side of the central headland (Figures 5C–5F) evidences that the tidal currents provide a minor forcing compared to the discharge of the Ribeira de Iguape River, the largest fluvial course in SE Brazil. Furthermore, these observations are evidence that the hydraulic blockage was mainly due to the Ribeira de Iguape flow, with a minor influence of the tidal currents. Therefore, in accordance with previous studies (Aubrey and Gaines, 1982; Kunte and Wagle, 1991; Avinash *et al.*, 2013; Hedge *et al.*, 2015), longshore drift is essential for the formation and elongation of spits in microtidal river mouths, but the river drift plays a significant role in the growth, morphology and possible degradation of the baymouth spits.

Simultaneously, due to these morphological changes in both the Jureia Beach spit and the central spit, the southeastward migration of the river mouth eroded a large sector of the headland. This erosion exposed the Pleistocene deposits. The shoreline retreated 386.7 m in 37 years, i.e. at a rate of 10.45 m/yr. High rates of erosion were also identified in the beaches of the Comprida Island spit, with a retreat rate of 10 m/yr deduced from a one-year survey (Silva *et al.*, 2014). However, considering the previous studies for the region (Tessler *et al.*, 2006; Mahiques *et al.*, 2016), it is clear that the shoreline retreat of the Iguape headland during the last decades to centuries represents the highest erosion rates of the entire São Paulo Bight. Because of this substantial erosion, the common mouth of the Ribeira de Iguape River and the Icapara Inlet was flanked by baymouth spits in 2009, i.e. the Jureia Beach spit and Comprida Island spit.

The longshore migration rates of the Comprida Island spit in recent decades, considering only the initial and final stage

(Table III), are approximately equal to those obtained by Nascimento *et al*. (2008) but lower than those from 1882 to 1964 related to the stronger influence of the artificial Valo Grande channel in Icapara Inlet; the Valo Grande channel was still widening and therefore had greatly fluctuating discharge (Geobrás, 1966). Kawakubo (2009), based on only four satellite images, indicated lower migration rates for the Comprida Island spit, but similar values to those obtained in the present work for the Jureia Beach spit. Kawakubo (2009) ended their study in 2000, so perhaps the discrepancy is because the system had already recovered from the changes induced by the strong river discharge of 1983. Additionally, considering these migration rates and intervals, as well as the initial distance in 1721 of 8.3 km between the river mouth and tidal inlet (Pimentel, 1762), it can be deduced that the width of the headland decreased approximately 3.1 km from 1721 to 1882, 2.6 km from 1882 to 1964 (Geobras, 1966), 0.3 km from 1964 to 1976 (Nascimento *et al*., 2008) and 1.8 km from 1976 to 2009 (Table III and Figure 6). Then, from 1721 to 1882, the average migration rate was 21.1 m/yr; for the period from 1721 to 2009, the width of the headland decreased 7.8 km, which corresponds to a longshore migration rate of 27.0 m/yr. The migration rate during the initial formation of the Comprida Island barrier spit, from 6000 to 5000 BP, were 10.2 to 22.8 m/yr (Guedes, 2009). These rates confirm that the highest migration rate corresponded to the intermediate interval, when the Valo Grande channel was widening (Nascimento *et al*., 2008).

However, the analysis of only the initial and final stages does not describe the migration behaviour of the spits. In contrast, the analysis of the series of images allows detailed information about the decadal and seasonal shoreline changes to be obtained (Aubrey and Gaines, 1982; Frihy and Lawrence, 2004; Avinash *et al*., 2013; Hedge *et al*., 2015). The mean migration rates (Table IV) have shown more complex dynamics of the bedforms related to the Ribeira de Iguape River mouth, in contrast with the more static dynamics of the processes in the Icapara Inlet (Table III). Therefore, mean migration rates are actually more significant in the characterization of the coastal processes and bedforms migration than the total migration rates. The mean migration rates definitively confirm that the river flow and hydraulic blockage are very important in the recent Ribeira de Iguape River mouth evolution, as proposed by Bentz and Giannini (2003), while it is a minor factor in the Icapara Inlet and the Comprida Island spit evolutions during the last decades, in contrast with the hydrodynamic control of the Valo Grande channel and the Icapara Inlet in previous decades (Nascimento *et al*., 2008).

The two strongest El Niño events from 1951 to 2017 are clearly related to the most substantial morphological changes in the system. The first event, in 1982–1983, is mainly related to high erosion by punctual, extreme rainfall; the second event, in 1997–1998, is related to the hydraulic blockage by the high river flow during several years. The merge of the Ribeira de Iguape River mouth and Icapara Inlet could be also related to high fluvial erosion during the El Niño events, but the headland erosion was primarily the result of a long-term convergent migration of both the drainage systems over decades and even centuries (Geobrás, 1966; Nascimento *et al*., 2008; Guedes *et al*., 2011). Many studies have reported the influence of the El Niño events of 1982–1983 and 1997–1998 (O'Neil, 1987; Komar, 1986, 1998; Komar *et al*., 1989; Peterson *et al*., 1990; Correa and González, 2000; Restrepo *et al*., 2002; Allan *et al*., 2003; Hepner and Davis, 2004) and other interannual climatic oscillations (Morales *et al*., 2006; Nahon *et al*., 2015) in the spit evolution. However, this is the first study that relates these climatic oscillations to the formation, evolution and disappearance of baymouth spits.

However, it has been reported that the formation of several mouths in a single delta is related to smaller waves (Nardin *et al*., 2013), while larger waves suppress mouth formation (Jerolmack and Swenson, 2007; Syvitski and Saito, 2007; Geleynse *et al*., 2011). Similarly, the closure of the channels in the Ribeira de Iguape River mouth between each of the emerged sand banks and the mainland is evidence of a significant influence of the waves and the associated longshore drift. Thus, neither channel was the result of a river flow cutting the spit, instead, the sand banks separated in a width river mouth configuration and later, the channels were closed by longshore drift (Figures 5C–5F and 6).

The wave and microtidal regimes allow classification of the area as wave-dominated, according to the Hayes (1979) scheme. In a wave-dominated coast, bypassing of sediments occurs across the river mouth (Zenkovich, 1967). After Nienhuis *et al*. (2016), the fraction of the longshore drift that is bypassed and the size of the river mouth spit control the alongshore migration rate of the river mouths. The Comprida Island sand barrier, which is a sandy barrier spit according to Otvos (2012), currently extends for 65 km, while the Jureia Beach spit is approximately 4 km long. However, the magnitude of the river erosion and river blocking in extreme events are so high that they generate not only a net southwestward longshore drift but also higher migration rates in the river mouth than in the Icapara Inlet; the initial migration rates were faster and high rainfall events related to El Niño triggered high rates of forward and setback spit migration (Table III).

Several mechanisms have been proposed for the formation of baymouth spits; all of the mechanisms are for regions with significant longshore drift, and they include a hydraulic blockage to explain the formation of the counter-drift spit. For tidal inlets, Lynch-Blosse and Kumar (1976) related the hydraulic blockage to the interaction between the strong tidal currents and the wave refraction; in river mouths, the hydraulic blockage has been related to the river flow (Aubrey and Gaines, 1982; Carr, 1986; Kunte and Wagle, 1991). The geomorphological evolution of the area allows the identification of two new conceptual models for the formation of baymouth spits, at least for river mouths in humid tropical, microtidal, wave-dominated coasts. The first model is for a single mouth. Erosion of the spit by both, high river flow (Figure 5B) and waves, the subsequent formation and emersion of a sand bank (Figure 5C) constituted by sediments of the eroded spit, and finally the attachment of the sand bank to the opposite flank of the river mouth, which forms the second spit (Figure 5D). However, if the dominant littoral drift does not develop this new spit due to the dominance of the hydraulic blockage, this spit can be degraded (Figures 5E–5G). This model is similar to those described for other river mouths in microtidal coasts (Aubrey and Gaines, 1982; Carr, 1986; Kunte and Wagle, 1991). However, in previous models there is initially a down-drift spit, and later, the counter-drift spit is developed by the hydraulic blockage; in addition, the counter-drift spit can disappear when the hydraulic blockage decreases due to a change in the tidal currents or the river flow (Lynch-Blosse and Kumar, 1976; Aubrey and Gaines, 1982). In contrast, in this first new model, the counter-drift spit forms before that of the down-drift spit, which is formed and disappears within approximately a decade, due to the high intensity of the hydraulic blockage and the low intensity of the dominant longshore drift. This model is forced by El Niño events.

The second model identified for the formation of baymouth spits in the study area is valid when two isolated and deflected river mouths are contiguous. The first river mouth, joined in this

case with a microtidal inlet, is migrating in the same direction as the dominant littoral drift; the second river mouth is migrating in the opposite direction due to the intense hydraulic blockage from a higher river discharge rate. The convergent alongshore migration of both river mouths allows them to merge, and consequently, their associated spits became baymouth spits (Figures 5G and 5H). In this second model, even in the initial stage, the hydraulic blockage by the river mouth is more influential that the fluvial erosion or other extreme event that could break the fronting mouth spit. However, this model is different to all the previously described models for the formation of baymouth spits, which are related to a single tidal inlet or river mouth; this new model is based on two convergent drainage systems with very different flow rates. In the area, one of the drainage systems is related to a large estuary controlled by microtidal currents and the other drainage system is related to a major river with higher discharge rates. The hydraulic blockage in the first drainage system is not relevant, while it is important throughout the year in the second drainage system. The present situation and geological inheritance suggest that the persistence of this baymouth spit should be expected to be longer than one to several decades.

The future geomorphological evolution of the present baymouth spits, as a result of the opposite migration trends of the Comprida Island spit, a 6000-year old barrier spit associated to the highest estuary of São Paulo Bight (Guedes, 2009; Giannini *et al.*, 2009; Guedes *et al.*, 2011), and the Jureia Beach spit, a several-decades old spit associated to the hydraulic blockage by the larger and wider river of São Paulo Bight (Bentz and Giannini, 2003), is currently uncertain. Nevertheless, if the southwestward migration of the river mouth overlays the northeastward migration of the inlet, the baymouth spits would persist, with the elongation of the Jureia Beach spit and alongshore retreat of the Comprida Island spit. In the opposite case, the elongation of the Comprida Island spit will continue and Jureia Beach spit will disappear, resulting again in a northeastward-detached mouth of the Ribeira de Iguape River. Nevertheless, the bimodal wave pattern and hydraulic blockage would favour the formation of a new counter-drift spit. Therefore, in both scenarios, it can be expected that baymouth spits will be in the area for a long time.

A similar wave and rainfall pattern occurs along the São Paulo Bight. Consequently, the mouths of the Itaguaré and Ubatumirim Rivers, at 177 and 297 km northeastward of the study area, respectively, as well as the southernmost mouth of the Cananéia Estuary, 96 km to the southwest of the study area, also have temporary baymouth spits. All these rivers have coastal plains with low human occupation and mangroves. Their river mouths are deflected by spits and they are not constrained by the rocky outcrops of the Serra do Mar mountain chain, in contrast with many other rivers in the region. The analysis of their geomorphological evolution is currently in progress. Nevertheless, the baymouth spits associated with Comprida Island and Jureia Beach are the most extensive and therefore the most representative example in the region.

The high sediment supply of the suspended, fine sediments to the littoral water can be observed in the satellite images and aerial photographs of the Ribeira de Iguape River mouth and other minor rivers. The true volume of the fluvial sediment supply is unknown and the bathymetric information near this drainage system is practically absent in the nautical charts. However, Bonetti-Filho and Furtado (1996) suggested that the changes in the submerged sand banks accompanied the evolution of the emerged bedforms. Therefore, the distribution of the sediments in the adjacent submerged areas should also be taken into consideration in future studies to completely understand and model this sedimentary system.

Development of symmetrical and asymmetrical baymouth spits have been obtained by numerical models (Uda and Serizawa, 2011; Watanabe *et al.*, 2014), although they ignore fluvial flows and tidal currents, consider only wave action, and include many other simplifications (Watanabe *et al.*, 2014). Simulation of the formation of baymouth spits has also been achieved by process-based numerical modelling (Nienhuis *et al.*, 2016). The São Paulo Bight, in general, and this study area, in particular, are ideal reference locations for future calibration and validation of models of baymouth spit formation and development. Future modelling work could be very useful to determine the future evolution of the spits and to define adequate coastal management measures.

Conclusions

Two successive configurations with baymouth spits were formed in recent decades, during the longshore convergence of the Ribeira de Iguape River mouth and Icapara Inlet. The bidirectional longshore drift and the hydraulic blockage of the Ribeira de Iguape River mouth, combined with a minor influence of the tidal currents in the Icapara Inlet, explain the convergent longshore migration of the spits and the outlets.

Formation and degradation of the first baymouth spits were associated with the bedforms developed due to the El Niño events of 1983, 1991–1993 and 1989–1999. High river flows during the extreme 1983 El Niño event eroded the inland side of the Jureia Beach spit, forming submerged sand banks. These sand banks attached to the Iguape headland in the southern flank of the river mouth, forming a new spit in 1989. Due to the dominant northeastward longshore drift, this new spit showed a convergent trend to the older northern spit. High erosion of the headland caused this spit to disappear in 2000. Therefore, in contrast to the previous model from the literature, in this scenario with high intensity of the hydraulic blockage and low intensity of the dominant longshore drift, the counter-drift spit was formed first, while the down-drift spit formed and disappeared within a decade.

The second configuration with baymouth spits formed in 2009, when continuous erosion of the central headland allowed the connection of the river mouth and Icapara Inlet; the associated Jureia Beach spit and Comprida Island barrier spit were converging at the margins of this area. This coastal configuration is still present. Similar to other microtidal wave-dominated coasts, the formation of these baymouth spits is controlled by the interaction of the bidirectional longshore drift and the river discharges. However, this model is the result of the convergence of two drainage systems, due to the geological setting of the region since 6000 BP, while all the previous studies are based on a single drainage system.

Acknowledgments—The authors thank the National Oceanic and Atmospheric Administration and the Instituto Nacional de Pesquisas Espaciais for providing the satellite images and the Departamento de Águas e Energia Elétrica of the State of São Paulo for supplying the river flow records. This study was partially funded by a pre-graduate scholarship of the University of Alicante. The authors are also indebted to Clement Poirier and an anonymous reviewer for their suggestions that helped to improve the manuscript and to José Enrique Tent and Dalton Sasaki for their collaboration. This study is a contribution to the research project HIGEOLAP funded by the FAPESP (ref. 2015/16067-2).

References

Alcántara-Carrió J, Sasaki DK, Mahiques M, Taborda R, Souza LAP. 2017. Sedimentary constraints on the development of a narrow deep

strait (São Sebastião Channel, SE Brazil). *Geo-Marine Letters* **37**(5): 475–488.

Allan JC, Komar PD, Priest G. 2003. Shoreline variability on the high-energy Oregon coast and its usefulness in erosion-hazard assessments. *Journal of Coastal Research, SI* **38**(special issue): 83–105.

Arnott RD. 2010. *Introduction to Coastal Processes and Geomorphology*. Cambridge University Press: New York 441 pp.

Ashton AD, Nienhuis J, Ells K. 2016. On a neck, on a spit: controls on the shape of free spits. *Earth Surface Dynamics* **4**: 193–210.

Aubrey DG, Gaines AG. 1982. Rapid formation and degradation of barrier spits in areas with low rates of littoral drift. *Marine Geology* **49**: 257–278.

Avinash K, Deepika B, Jayappa KS. 2013. Evolution of spit morphology: a case study using a remote sensing and statistical based approach. *Journal of Coastal Conservation* **17**: 327–337.

Bentz D, Giannini PCF. 2003. Interpretação aerofotogeomorfológica da planície costeira de Una-Juréia, municípios de Peruíbe-Iguape, SP: modelo evolutivo e origem da erosão na praia da Juréia. In IX Congresso da Associação Brasileira de Estudos do Quaternário (ABEQUA), 9, 5.

Besnard W. 1950. Considerações gerais em torno da região lagunar de Cananéia-Iguape, I. *Boletim do Instituto Paulista de Oceanográfico* **1**: 9–26.

Bonetti-Filho J, Conti LA, Furtado VV. 1996. Suspended sediment concentration variability and its relation to tidal currents in microtidal systems. *Academia Brasileira de Ciência* **68**: 485–494.

Bonetti-Filho JF, Furtado VV. 1996. Modelo digital de terreno aplicado ao estudo de feições costeiras submersas no litoral sul do Estado de São Paulo. *Geociências* **2**: 367–380.

Carr AP. 1986. The estuary of the river Ore, Suffolk: three decades of change in a longer-term context. *Field Studies* **6**: 439–458.

Correa ID, Alcántara-Carrió J, González RDA. 2005. Historical and recent shore erosion along the Colombian Caribbean coast. *Journal of Coastal Research* **49**(special issue): 52–57.

Correa ID, González JL. 2000. Coastal erosion and village relocation: a Colombian case study. *Ocean & Coastal Management* **43**: 51–64.

Dan S, Walstra DJR, Stive MJF, Panin N. 2011. Processes controlling the development of a river mouth spit. *Marine Geology* **280**(1): 116–129.

Davis RA. 2013. A new look at barrier-inlet morphodynamics. *Journal of Coastal Research* **69**: 1–12.

Dillenburg SR, Hesp PF. 2009. Coastal barriers — an introduction. In *Geology and Geomorphology of Holocene Coastal Barriers of Brazil*, Dilllenburg SR, Hesp PA (eds). Springer Publisher: New York; 1–15.

Eddison J. 1998. Catastrophic changes: the evolution of the barrier beaches of Rye Bay. In *Romney Marsh: Environmental Change and Human Occupation in a Coastal Lowland*, Eddison J, Gardiner M, Long AJ (eds). Oxford University Committee for Archaeology Monograph 46. Oxford University Committee for Archaeology: Oxford; 65–87.

Evans OF. 1942. The origin of spits, bars, and related structures. *The Journal of Geology* **50**(7): 846–865.

Frihy O, Lawrence D. 2004. Evolution of the modern Nile delta promontories: development of accretional features during shoreline retreat. *Environmental Geology* **46**: 914–931.

Geleynse N, Storms JEA, Walstra DJR, Jagers HRA, Wang ZB, Stive MJF. 2011. Controls on river delta formation; insights from numerical modelling. *Earth and Planetary Science Letters* **302**(1–2): 217–226.

Geobrás. 1966. *Geobrás S/A Engenharia e Fundações. Complexo Valo Grande, Mar Pequeno e Rio Ribeira de Iguape*. Relatório 2 vols. DAEE: São Paulo 448 pp.

Giannini PCF, Guedes CF, Nascimento DR, Jr, Tanaka APB, Angulo RJ, Assine ML, de Souza MC. 2009. Sedimentology and morphological evolution of the Ilha Comprida barrier system, southern São Paulo Coast. In *Geology and Geomorphology of Holocene Coastal Barriers of Brazil*, Dilllenburg SR, Hesp PA (eds). Springer Publisher: New York 380 pp.

Guedes CCF. 2009. *Evolução sedimentar quaternária da ilha comprida, estado de São Paulo*, Master Thesis. University of São Paulo; 147 pp.

Guedes CCF, Giannini PCF, Sawakuchi AO, DeWitt R, Nascimento DR, Aguiar VAP, Rossi MG. 2011. Determination of controls on Holocene barrier progradation through application of OSL dating: the Ilha Comprida Barrier example, southeastern Brazil. *Marine Geology* **285**: 11–16.

Hanamgond PT, Mitra D. 2008. Evolution of Malvan Coast, Konkan, west coast of India – a case study using remote sensing data. *Journal of Coastal Research* **24**(3): 672–678.

Hayes MO, Fitzgerald DM. 2013. Origin, evolution, and classification of tidal inlets. *Journal of Coastal Research*, SI **69**: 14–33.

Hayes MO. 1979. Barrier island morphology as a function of wave and tide regime. In *Barrier Islands from the Gulf of St. Lawrence to the Gulf of Mexico*, Leatherman SP (ed). Academic Press: New York; 1–27.

Hedge VS, Nayak SR, Krishnaprasad PA, Rajawat AS, Shalini R, Jayakumar S. 2015. Evolution of diverging spits across the tropical river mouths, central west coast of India. *Journal of Coastal Zone Management* **18**: 402.

Hepner TL, Davis RA. 2004. Effect of El Niño (1997–98) on beaches of the Peninsular Gulf Coast of Florida. *Journal of Coastal Research* **20**(3): 776–791.

Hesp PA, Maia LP, Claudio-Sales V. 2009. The Holocene barriers of Maranhão, Piauí and Ceará States, northeastern Brazil. In *Geology and Geomorphology of Holocene Coastal Barriers of Brazil*, Dilllenburg SR, Hesp PA (eds). Springer Publisher: New York; 325–345.

Hoan LX, Hanson H, Larson M, Kato S. 2011. A mathematical model of spit growth and barrier elongation: Application to Fire Island Inlet (USA) and Badreveln Spit (Sweden). *Journal of Estuarine, Coastal and Shelf Science* **93**: 468–477.

Hume TM, Herdendorf CE. 1993. On the use of empirical stability relationships for characterizing estuaries. *Journal of Coastal Research* **9**: 413–422.

Hume TM, Herdendorf CE. 1988. A geomorphic classification of estuaries and its application to coastal resource management – a New Zealand example. *Ocean & Shoreline Management* **11**: 249–274.

Jerolmack DJ, Swenson J. 2007. Scaling relationships and evolution of distributary networks on wave-influenced deltas. *Geophysical Research Letters* **34** L23402.

Johnson D. 1925. *The New England-Acadian Shoreline*. Wiley: New York 608 pp.

Kawakubo FS. 2009. Avaliação das mudanças na linha de costa na foz do rio Ribeira de Iguape/desembocadura lagunar Barra do Icapara (litoral sul de São Paulo – Brasil) utilizando dados do Landsat MSS, TM e ETM+. *Boletín del Instituto de Geografía, UNAM* **68**: 41–49.

Kidson C. 1963. The growth of sand and single spits across estuaries. *Zeitschrift für Geomorphologie* **7**(1–2): 177–201.

Komar PD. 1986. The 1982–83 El Nino and erosion on the coast of Oregon. *Shore & Beach* **54**(2): 3–12.

Komar PD. 1998. The 1997–98 El Niño and erosion on the Oregon coast. *Shore & Beach* **66**(3): 33–41.

Komar PD, Good JW, Shih SM. 1989. Erosion of Netarts Spit, Oregon: continued impacts of the 1982–83 El Niño. *Shore & Beach* **57**(1): 11–19.

Kraus NC. 1999. Analytical model of spit evolution at inlets. *Proceedings of Coastal Sediments ASCE* **99**: 1739–1754.

Kunte PD, Wagle BG. 1991. Spit evolution and shore drift direction along South Karnataka Coast, India. *Giornale di Geologia* **153**: 71–80.

Kuroiwa M, Matsubara Y, Suzuki Y, Kuchiishi T. 2014. Numerical model for predicting sand bar formation around river mouth. *Journal of Korean Society of Coastal and Ocean Engineers* **26**(2): 96–102.

Liu H. 2013. Dynamic changes of coastal morphology following the 2011 Tohoku tsunami. *APAC (Asian Pacific Conference)* **26**: 594–601.

Lovegrove H. 1953. Old shorelines near Camber Castle. *Geographical Journal* **119**: 200–207.

Lynch-Blosse M, Kumar N. 1976. Evolution of downdrift-offset tidal inlets: a model based on the Brigantine Inlet system of New Jersey. *The Journal of Geology* **84**(2): 165–178.

Mahiques MM, Burone L, Figueira RCL, Lavenére-Wanderley AAO, Capellari B, Rogacheski CE, Barroso CP, Santos LAS, Cordero LM, Cussioli MC. 2009. Anthropogenic influences in a lagoonal environment: a multiproxy approach at the Valo Grande mouth, Cananéia-Iguape system (SE Brazil). *Brazilian Journal of Oceanography* **57**(4): 325–337.

Mahiques MM, Figueira RCL, Alves DP, Italiani DM, Martins CC, Dias JMA. 2014. Coastline changes and sedimentation related with the opening of an artificial channel: the Valo Grande Delta, SE Brazil. *Anais da Academia Brasileira de Ciências* **84**: 1597–1607.

Mahiques MM, Figueira RLC, Salaroli AB, Alves DPV, Gonçalves C. 2013. 150 years of anthropogenic metal input in a Biosphere Reserve: the case study of the Cananéia-Iguape coastal system, southeastern Brazil. *Environmental Earth Sciences* **68**(4): 1073–1087.

Mahiques MM, Siegle E, Alcántara-Carrió J, Silva FG, Sousa PHGO, Martins CC. 2016. The beaches of the state of São Paulo. In *Brazilian Beach Systems*, Short AD, Klein AHF (eds). Springer: Cham; 397–418.

Martin L, Suguio K. 1979. Le Quaternaire Marin du littoral brésilien entre Cananéia et Barra de Guaratiba (RJ). In *Proceedings of the International Symposium on coastal evolution in the Quaternary*. IGCP: São Paulo; 296–331.

Masselink G, van Heteren S. 2014. Response of wave-dominated and mixed-energy barriers to storms. *Marine Geology* **352**: 321–347. https://doi.org/10.1016/j.margeo.2013.11.004.

Mesquita AR, Harari J. 1983. *Tides and Tide Gauges of Cananéia and Ubatuba-Brazil (24°)*. Internal Report Instituto Oceanográfico of the University of São Paulo 11. Instituto Oceanográfico: São Paulo; 1–14.

Morales JA, Cantano M, Rodríguez-Ramírez A, Martín BR. 2006. Mapping geomorphology and active processes on the coast of Huelva (southwestern Spain). *Journal of Coastal Research* **48**(special issue): 89–99.

Muehe D. 2012. O litoral brasileiro e sua compartimentação. In *Geomorfologia do Brasil*, Cunha SB, Guerra AJT (eds), 8th edn. Bertrand Brasil: Rio de Janeiro; 273–349.

Nagai HR, Sousa SHM, Mahiques MM. 2014. The southern Brazilian shelf. In *Continental Shelves of the World: Their Evolution during the Last Glacio-Eustatic*, Chiocci FL, Chivas AR (eds). Geological Society: London; chapter 5; 47–54.

Nahon A, Idier, D, Fenies, H, Mugica J, Senechal N, Mallet C. 2015. Role of North Atlantic climate variability on barrier-spit oscillations: the cap ferret. *Proceedings of Coastal Sediments 2015*.

Nardin W, Mariotti G, Edmonds DA, Guercio R, Fagherazzi S. 2013. Growth of river mouth bars in sheltered bays in the presence of frontal waves. *Journal of Geophysical Research - Earth Surface* **118**: 872–886.

Nascimento DR. 2006. *Morfologia e Sedimentologia ao Longo do sistema Praia-Duna Frontal de Ilha Comprida, SP*, Unpublished Undergraduate Thesis. University of São Paulo.

Nascimento DR, Giannini PCF, Tanaka APB, Guedes CCF. 2008. Mudanças morfológicas da extremidade NE da Ilha Comprida (SP) nos últimos dois séculos. *Revista do Instituto de Geociências-USP* **8**: 25–39.

Nienhuis JH, Ashton AD, Nardin W, Fagherazzi S, Giosan L. 2016. Alongshore sediment bypassing as a control on river mouth morphodynamics. *Journal of Geophysical Research - Earth Surface* **121**: 664–683.

Nimer E. 1989. *Climatologia do Brasil*, second edn. IBGE: Rio de Janeiro 421 pp.

O'Brien MP. 1969. Equilibrium flow areas of inlets on sandy coasts. *Journal of the Waterways, Harbors, and Coastal Engineering Division of the American Society of Civil Engineers* **95**: 43–52.

O'Neil DJ. 1987. *Variations in Alsea River Flow; Implications for Alsea Spit & Inlet Instability*. Unpublished MSc Thesis: Oregon State University, Corvallis, OR 32 pp.

Ollerhead J. 1993. *The Evolution of Buctouche Spit, New Brunswick, Canada*, PhD Thesis. University of Guelph, 156 pp.

Orejarena Rondón AF, Afanador Franco F, Ramos de la Hoz I, Conde Frías M, Restrepo López JC. 2015. Evolución morfológica de la espiga de Galerazamba, Caribe colombiano. *Boletín Científico CIOH* **33**: 123–144.

Otvos EG. 2012. Coastal barriers – nomenclature, processes, and classification issues. *Geomorphology* **139–140**: 39–52.

Palalane J, Larson M, Hanson H. 2014. Analytical model of sand spit evolution. Analytical model of sand spit evolution. *Proceedings of the 34th International Conference on Coastal Engineering*, Seoul, South Korea, ASCE.

Peterson CD, Jackson PL, O'Neil DJ, Rosenfeld CL, Kimerling AJ. 1990. Littoral cell response to interannual climate forcing 1983–1987 on the Central Oregon coast, USA. *Journal of Coastal Research* **6**(1): 87–110.

Pianca C, Mazzini PLF, Siegle E. 2010. Brazilian offshore wave climate based on NWW3 reanalysis. *Brazilian Journal of Oceanography* **58**: 53–70.

Pimentel M. 1762. Arte de navegar em que se ensinão as regras praticas, e os modos de cartear, e de graduar a balestilha por via de números e muitos problemas uteis à navegação, e roteiro das viagens, e costas marítimas de Guiné, Angola, Brazil. Indias, e Ilhas Occidentais, e Orientaes: Lisboa; 603 pp.

Raghavan BR, Vinod BT, Dimple KA, Prabhu HV, Udayashankar HN, Muthy TRS. 2001. Evaluation of the Nethravathi spit complex, west coast of India: integrated change detection study using topographic and remotely sensed data. *Indian Journal of Marine Sciences* **30**(4): 268–270.

Redfield AC, Rubin M. 1962. The age of salt marsh peat and its relation to sea level at Barnstable, Massachusetts. *Proceedings of the National Academy of Science* **48**: 1728–1735.

Restrepo JD, Kjerfve B, Correa ID, González J. 2002. Morphodynamics of a high discharge tropical delta, San Juan River, Pacific coast of Colombia. *Marine Geology* **192**: 355–381.

Robinson AHW. 1955. The harbor entrances of Poole, Christchurch and Pagham. *Geographical Journal* **121**: 33–50.

Santos SCL. 2005. *Um modelo de banco de dados geográficos para a resposta do litoral paulista*, Unpublished PhD Thesis. University of São Paulo; 216 pp.

Schwartz ML. 1972. *Spits and Bars*. Dowden, Hutchinson & Ross: Stroudsberg 452 pp.

Silva FG, Sousa PHGO, Siegle E. 2016. Longshore transport gradients and erosion processes along the Ilha Comprida (Brazil) beach system. *Ocean Dynamics* **66**(6–7): 853–863.

Silva FG, Sousa PHGO, Siegle E. 2014. Wave climate analysis and its relation with erosion processes along the beach system of Ilha Comprida (SP), Brazil. *Proceedings of the 17th Physics of Estuaries and Coastal Seas (PECS) Conference*, Porto de Galinhas, Brazil.

Suguio K, Martin L. 1978. Formações quaternárias marinhas do litoral paulista e sul fluminense. In: Internacional Symposium on Coastal Evolution in the Quaternary, São Paulo, SBG/IGUSP, Special Publication, 1, 55p.

Suguio K, Martin L. 1976. Presença de tubos fósseis da "Callianassa" nas formações quaternárias do litoral paulista e sua utilização na reconstrução ambiental. *Boletín del Instituto de Geociências* **7**: 17–26.

Syvitski JPM, Saito Y. 2007. Morphodynamics of deltas under the influence of humans. *Global and Planetary Change* **57**: 261–282.

Tessler MG, Mahiques MM. 1993. Utilization of coastal geomorphic features as indicators of longshore transport: examples of the southern coastal region of the State of São Paulo, Brazil. *Journal of Coastal Research* **9**(3): 823–830.

Tessler MG. 1982. *Sedimentação atual na região lagunar de Cananéia-Iguape, Estado de São Paulo*, Master's Thesis. University of São Paulo; 121 pp.

Tessler MG, Cazzoli y Goya S, Yoshikawa PS, Hurtado SN. 2006. São Paulo. In *Erosão e progradação do litoral brasileiro*, Muehe D (ed). Ministério de Médio Ambiente: Brasilia; 297–346.

Tessler MG, Furtado V. 1983. Dinâmica de sedimentação das feições de assoreamento da região lagunar Cananéia–Iguape, Estado de São Paulo. *Boletim do Instituto Paulista de Oceanografia* **32**(2): 117–124.

Tolman HL, Balasubramaniyan B, Burroughs LD, Chalikov DV, Chao YY, Chen HS, Gerald VM. 2002. *Development and Implementation of Wind-generated Ocean Surface Wave Models at NCEP*. NCEP Notes 17. American Meteorological Society: Washington, DC; 311–333.

Trenberth K. 1983. What are the seasons? *Bulletin of the American Meteorological Society* **64**: 1276–1282.

Uda T, Serizawa M. 2011. Model for predicting formation of bay barriers in flat shallow sea. *Proceedings of the Coastal Sediments '11*; 1176–1189.

van Maren DS. 2005. Barrier formation on an actively prograding delta system: the Red River Delta, Vietnam. *Marine Geology* **224**: 123–143.

Vera AR, Vigliarolo PK, Berbery EH. 2002. Cold season synoptic scale waves over subtropical South America. *Monthly Weather Review* **130**: 684–699.

Vital H. 2009. The mesotidal barriers of Rio Grande do Norte. In *Geology and Geomorphology of Holocene Coastal Barriers of Brazil*, Dilllenburg SR, Hesp PA (eds). Springer Publisher: New York; 289–323.

Ward EM. 1922. *English Coastal Evolution*. Methuen & Company: London 105 pp.

Watanabe S, Uda T, Serizawa M, Miyahara S. 2014. Numerical simulation of elongation and merging of bay mouth sand spits using the BG model. *Proceedings of the 34th Conference on Coastal Engineering*, Seoul, Korea.

Wolter K, Timlin MS. 1993. Monitoring ENSO in COADS with a seasonally adjusted principal component index. In *Proceedings of the 17th Climate Diagnostics Workshop*. Climatology Survey, CIMMS and the School of Meteorology, University of Oklahoma: Norman, OK; 52–57.

Zembruscki SG. 1979. Geomorfologia da margem continental sul brasileira e das bacias oceânicas adjacentes. In *Geomorfologia da margem continental brasileira e das áreas oceânicas adjacentes*, Chaves HAF (ed). Série Projeto REMAC, 7. PETROBRAS: Rio de Janeiro; 129–177.

Zenkovich VP. 1967. *Processes of Coastal Development*. Wiley-Interscience: New York 751 pp.